






Original Research

tiRNA-Gln-CTG is Involved in the Regulation of Trophoblast Cell Function in Pre-eclampsia and Serves as a Potent Biomarker

Yixiao Wang^{1,†}, Xiaohong Ji^{2,†}, Hengmei Shi², Sicong Liu¹, Hong Yu^{1,*}

¹Department of Obstetrics and Gynecology, Zhongda Hospital, School of Medicine, Southeast University, 210000 Nanjing, Jiangsu, China

²Department of Obstetrics and Gynecology, Women's Hospital of Nanjing Medical University, Nanjing Women and Children's Healthcare Hospital, 210000 Nanjing, Jiangsu, China

*Correspondence: yuhong@seu.edu.cn (Hong Yu)

†These authors contributed equally.

Academic Editor: Indrajit Chowdhury

Submitted: 30 August 2024 Revised: 23 November 2024 Accepted: 29 November 2024 Published: 21 January 2025

Abstract

Background: Pre-eclampsia (PE) is a gestational disorder that significantly endangers maternal and fetal health. Transfer ribonucleic acid (tRNA)-derived small RNAs (tsRNAs) are important in the progression and diagnosis of various diseases. However, their role in the development of PE is unclear. Consequently, we detected the expression profiles of tsRNAs in the plasma of patients with PE as well as those in the plasma of the healthy control group, and a multiplicity of experiments were conducted with the aim of clarifying their roles in the occurrence and development of PE and the feasibility of serving as predictive biomarkers for this disorder. **Methods:** High-throughput sequencing of tsRNA in plasma from PE cases was performed to evaluate its potential as a diagnostic or therapeutic biomarker. The function of tsRNA in trophoblasts was explored using the HTR-8/SVneo cell line. Plasma from pregnant women with suspected PE was analyzed to assess the potential of tsRNA to act as a predictive marker of PE. **Results:** High-throughput sequencing of tsRNA was performed on plasma from pregnant women with PE and from healthy pregnant controls. Analysis revealed a significant reduction in the level of tRNA-derived stress-inducing RNA (tiRNA)-Gln-CTG in the plasma ($p < 0.001$) and placenta ($p < 0.001$) of pregnant women with PE, suggesting its potential involvement in the development of this condition. tiRNA-Gln-CTG was identified in the cytoplasm and nucleus of HTR-8/SVneo cells. *In vitro* experiments revealed that tiRNA-Gln-CTG influences the proliferation, cycling, migration, and invasion of HTR-8/SVneo cells, possibly by targeting the 3' UTR region of thrombospondin-2 messenger ribonucleic acid (mRNA) for degradation. Extracellular vesicle (EV) carriers may mediate the level of tiRNA-Gln-CTG in the circulation. Y-box binding protein-1 (YBX1) may be involved in loading tiRNA-Gln-CTG into EVs. The sensitivity of low tiRNA-Gln-CTG levels for predicting the onset of PE in suspected cases was 91.7% within 1 week of delivery, 85.7% within 4 weeks of delivery, and 89.3% before delivery, with corresponding specificities of 84.5%, 79.2%, and 73.4%, respectively. **Conclusions:** tiRNA-Gln-CTG significantly influences trophoblast function and is associated with the development of PE. It can serve as an effective biomarker for predicting PE progression within one week of delivery in women with suspected PE.

Keywords: tRNA-derived small RNA; tiRNA-Gln-CTG; pre-eclampsia; biomarker

1. Introduction

Pre-eclampsia (PE) is a complex disorder that affects multiple systems during pregnancy. It has a critical effect on maternal mortality and morbidity, as well as on perinatal mortality [1,2]. PE is characterized by abnormal perfusion of the placenta, resulting in the release of soluble factors into the bloodstream. This leads to endothelial damage within the maternal vasculature, ultimately causing hypertension and multi-organ impairment. Low-dose aspirin prophylaxis reduces the risk of preterm PE. However, once PE is diagnosed the only effective treatment is labor induction and delivery, since there is no medication that prevents the progression of this condition [3]. The widely accepted 'two-stage' theory of PE pathogenesis involves, (1) inadequate spiral-artery remodeling due to reduced trophoblast invasion, and (2) systemic vascular damage from placental hypoperfusion [4]. It is therefore crucial to identify predic-

tive diagnostic markers and therapeutic targets based on this pathogenesis.

Transfer ribonucleic acid (tRNA)-derived small RNA (tsRNA) is a novel type of small noncoding RNA (sncRNA) that has recently been identified thanks to advances in high-throughput sequencing and bioinformatics analyses. tsRNA is categorized into tRNA-derived fragments (tRF) and tRNA-derived stress-inducing RNA (tiRNA, or tRNA-half) based on the cleavage site and length [5]. tRFs, including 5-tRF, 3-tRF, 1-tRF, and i-tRF, are 14–30 nucleotide sequences derived from mature or precursor tRNAs. Under conditions of stress, the mature tRNA anticodon loop is predominantly cleaved, producing 5'-half and 3'-half tiRNAs that are 29–50 nucleotides in length [6–8]. Emerging evidence indicates that tsRNAs influence the progression of disease and cancer by participating in biological processes such as gene silencing and protein translation [5,9].



tsRNA is considered to be a potential biomarker of various diseases, including acute myeloid leukemia [10], lupus nephritis [11], and lung cancer [12]. Furthermore, tsRNA has been shown to play a role in the development of colorectal [13], gastric [14], and breast [15] cancer. Maternal immune activation significantly alters tsRNA expression at the maternal-fetal interface in mice [16]. Palmitic acid treatment significantly reduces tRNA-Gly-derived tiRNA levels in trophoblast cells, thereby influencing the regulation of trophoblast apoptosis [17]. In addition, alterations in tissue tsRNA expression levels lead to changes in circulating tsRNA constitutive profiles. The investigation of tsRNA expression levels as potential biomarkers and therapeutic targets for PE may therefore be of great clinical value.

We conducted tsRNA sequencing on plasma samples from both pre-eclamptic and healthy pregnant women to identify differentially expressed tsRNAs. We then analyzed plasma from patients with suspected PE to validate candidate tsRNAs with the highest diagnostic potential for this condition. Bioinformatics analysis and multiple experimental approaches were employed to investigate the possible biological functions of tsRNAs in the development of PE, together with the underlying biological mechanisms. We identified tiRNA-Gln-CTG as a candidate tsRNA with notably reduced expression in placental trophoblasts and plasma of women with PE. Its contribution to PE development appears to be via its regulation of thrombospondin-2 (THBS2) protein expression. Exploration of the role and mechanism of tsRNAs in PE development is a promising new research direction for the diagnosis and treatment of this condition.

2. Methods and Materials

2.1 Participants, and Collection of Plasma and Placental Tissue

Six patients with PE and 6 healthy pregnant control patients were recruited from June 2022 to December 2023. The plasma from three PE patients and three healthy controls was used for high-throughput sequencing of tRF and tiRNA, while the plasma and placental trophoblast tissues of three other PE patients and three healthy controls were used to verify the consistency of tsRNA expression levels. To assess the potential of tsRNA as a predictive biomarker for PE, plasma samples were also collected from 150 patients with suspected PE, of which 28 did not give birth in our hospital. Consequently, the study analyzed 122 patients with suspected pre-eclampsia (PE). Given the documented 20% incidence of PE in women who are suspected of having this condition [18], the tiRNA-Gln-CTG biomarker was anticipated to reach 80% sensitivity and specificity, with $Z = 1.96$. The minimum sample size required was therefore calculated as: $n = 1.96^2 \times 0.2 \times (1 - 0.2)/0.2^2$, corresponding to a minimum sample size of 62. PE was diagnosed according to the 2020 ACOG Clinical Guidelines [19], and suspected PE according to previously reported criteria [18,20].

2.2 tRF and tiRNA Sequencing and Data Analysis

For high-throughput sequencing, plasma total RNA was first extracted using TRIzol reagent (15596026CN, Invitrogen, Carlsbad, CA, USA) as per the manufacturer's guidelines. It was then quantified using a NanoDrop-1000 (ND-1000, ThermoFisher Scientific, Waltham, MA, USA) instrument. The rtStar™ tRF & tiRNA Preprocessing Kit (AS-FS-005, Arraystar, Rockville, MD, USA) was used to eliminate RNA modifications that hinder the formation of small RNA sequencing libraries, including the removal of 3'-amino acids and 3'-cyclic phosphate for 3'-adaptor ligation, phosphorylation of 5'-OH to 5'-P for 5'-adaptor ligation, and demethylation of m1A and m3C. Sequencing libraries were prepared from pretreated total RNA in the following steps: (1) ligation of 3'-adaptors; (2) ligation of 5'-adaptors; (3) synthesis of complementary deoxyribonucleic acid (cDNA); (4) amplification via polymerase chain reaction (PCR); and (5) identification of PCR-amplified fragments within the size range of 134–160 bp. The amplified cDNA libraries were quantitatively analyzed using an Agilent 2100 Bioanalyzer (G2939A, Agilent, Santa Clara, CA, USA), and tsRNA high-throughput sequencing was performed with the Illumina NextSeq 500 system (NEXTSEQ 500, Illumina, San Diego, CA, USA). Following the generation of raw sequencing data, mature tRNA libraries were prepared by removing intronic sequences and appending 'CCA' to the 3' end. FastQC was used to assess sequencing quality. 5'- and 3'-adapter bases were trimmed by Cutadapt through Illumina quality filters. Trimmed reads were then aligned, allowing only one mismatch with the mature tRNA sequence. Unmapped reads were subsequently aligned to the precursor tRNA sequence using Bowtie software (Version 1.3.0, The Johns Hopkins University, Baltimore, MD, USA), with only one mismatch permitted. The abundance of tRF and tiRNA was assessed using their sequencing counts, which were normalized to counts per million (CPM) aligned total reads [21].

2.3 Cell Line and Treatment

The HTR-8/SVneo cell line was obtained from Servicebio Technology Co., Ltd. (Wuhan, Hubei, China) and cultured in RPMI-1640 (G4535, Servicebio, Wuhan, Hubei, China) with 10% fetal bovine serum (FBS, Gibco, Rockville, MD, USA) at 37 °C and in 5% CO₂. Cell lines underwent short tandem repeat (STR) profiling for validation and tested negative for mycoplasma. The HTR-8/SVneo PE-like hypoxia model was developed using 100 μM cobalt chloride hexahydrate (CoCl₂·6H₂O, C106772, Aladdin, Shanghai, China) as described previously [22]. Whether the construction of the hypoxia model of HTR-8/SVneo cells was successful was verified by detecting hypoxia-inducible factor-1α (HIF-1α) through Western blot (WB) assay.

2.4 RNA Extraction and qRT-PCR

RNA was extracted from cells, plasma, and placenta using TRIzol reagent, and its quality and quantity assessed using the NanoDrop-1000. Quantitative real-time PCR (qRT-PCR) was performed using the StepOnePlus Real-Time PCR System from Applied Biosystems (ThermoFisher Scientific, Waltham, MA, USA). The tsRNA was synthesized using the non-human-derived spike-in microRNA (miRNA) cel-miR-39-3p (miRA0000010-1, Ribobio, Guangzhou, Guangdong, China) as an exogenous reference for normalization in plasma, and RNU6B (U6, Ribobio, China) as an endogenous reference for normalization in placenta. Standardization of the messenger RNA (mRNA) level in cells was achieved using β -actin. The relative RNA expression was calculated by $2^{-\Delta\Delta CT}$. The primer sequences used for human *THBS2* were: forward, 5'-GACACGCTGGATCTCACCTAC-3' and reverse, 5'-GAAGCTGTCTATGAGGTCGCA-3'. The primer sequences for human β -actin were: forward, 5'-CATGTACGTTGCTATCCAGGC-3' and reverse, 5'-CTCCTTAATGTACGCACGAT-3'. Primers for tsRNA reverse transcription and PCR were provided by Ribobio, Guangdong, China. Detailed information and samples can be provided by e-mail at marketing@ribobio.com.

2.5 Cell Transfection

HTR-8/SVneo cells were seeded into 6-well plates and incubated in complete medium for 24 h until reaching 60–70% confluence. They were then transfected with a negative control (NC, sequence: GUUGUAGCUC-CGAAUUGCCGUUCAUGUUGGGA), a tiRNA-Gln-CTG mimic (sequence: GGUUCCAUGGUGUAAUG-GUUAGCACUCUGGACUC), or a tiRNA-Gln-CTG inhibitor (sequence: GAGUCCAGAGUGCUAACCAUUA-CACCAUGGAACC). All sequences were obtained from Ribobio (China) and were added with 200 μ L Opti-MEM (31985070, ThermoFisher Scientific, Waltham, MA, USA) and 5 μ L Lipofectamine 3000 (L3000015, ThermoFisher Scientific, Waltham, MA, USA) to transiently transfect HTR-8/SVneo cells. Subsequent experiments were performed 24–48 h after cell transfection. Detailed information and samples can be requested from Ribobio by e-mail (marketing@ribobio.com). Negative control (NC, UUCUCCGAACGUGUCACGUTT), *THBS2* small interfering (siRNA, GUACCUGCAAGAAAUU-UAATT), and Y-box-binding protein 1 (*YBX1*) siRNA (GGAGGCAGCAAUGUUACATT) were obtained from GenePharma (Shanghai, China) and transfected into HTR-8/SVneo cells using Lipofectamine 3000 as per the manufacturer's guidelines.

2.6 Analysis of tRF/tiRNA Functionality

TargetScan (<https://www.targetscan.org>) and miRanda (<https://anaconda.org/bioconda/miranda>) [23] were employed to predict target genes for the selected

tRFs/tiRNAs. Gene Ontology (GO) and Kyoto Encyclopedia of Genes and Genomes (KEGG) enrichment analyses were conducted using Metascape bioinformatics resources (<https://metascape.org>) [24], followed by an investigation of gene/protein interactions through the String database (<https://string-db.org>) [25].

2.7 CCK-8 Assay for the Measurement of Cell Proliferation

At 24 h after transfection, HTR-8/SVneo cells were seeded into 96-well plates at a density of 3000 cells per well. After incubating for 12, 24, and 48 h, 10 μ L of CCK-8 reagent (CK04, Dojindo, Kumamoto Prefecture, Japan) was added to each well. Following 2 h of incubation, the optical density at 450 nm was analyzed using a multifunctional enzyme marker (SynergyTM 4, Biotek, Winooski, VT, USA).

2.8 5-Ethynyl-2'-deoxyuridine (EdU) Proliferation Assay

At 24 h after transfection, HTR-8/SVneo cells were seeded at 10,000 per well in 96-well plates and cultured for 24 h. The EdU proliferation assay was carried out as per the manufacturer's guidelines (G1601, Servicebio, Wuhan, Hubei, China), and the proportion of cells that incorporated EdU was ascertained by fluorescence microscopy (Zeiss, Oberkochen, BW, Germany). The cell proliferation rate (%) = the number of positive cells (green fluorescence) / the number of total cells (blue fluorescence).

2.9 Flow Cytometry

Analysis of cell apoptosis. Cells were transfected, digested with EDTA-free trypsin, washed twice with phosphate-buffered saline (PBS), and then processed as per the manufacturer's guidelines (40310ES60, YEASON, Shanghai, China). Subsequently, apoptosis was assessed using flow cytometry (Attune NxT, Thermo Fisher Scientific, USA).

Analysis of the cell cycle. Transfected cells were digested, washed twice with PBS, and then processed as per the manufacturer's guidelines (40301ES60, YEASON, Shanghai, China). At the completion of treatment, flow cytometry was used to analyze the cell cycle (Attune NxT, Thermo Fisher Scientific, Waltham, MA, USA).

2.10 Wound Healing Assay

Transfected HTR-8/SVneo cells were cultured in 6-well plates until they were fully confluent. Scratch wounds were then created using a 200 μ L pipette tip, and three points were randomly marked. After washing the 6-well plates with PBS to eliminate dead cells, 2 mL of RPMI 1640 medium without FBS was added. Images were taken at designated sites at 0, 24, and 48 h post-incubation and analyzed with Image J software (Version 1.8.0, National Institutes of Health, Bethesda, MD, USA) to determine the wound area and calculate the healing rate. The wound healing rate

was determined by subtracting the wound area at 24 or 48 h from the initial wound area (0 h), then dividing by the initial wound area.

2.11 Transwell Assay

Cell migration assay. A total of 30,000 HTR-8/SVneo cells and 200 μ L of FBS-free RPMI 1640 medium were introduced into the upper chamber of a Transwell (3422, Corning, Steuben County, New York, USA). Simultaneously, 700 μ L of RPMI 1640 medium with 10% FBS was added to the lower chamber. Following removal of the culture medium from the upper chamber, samples were fixed with 700 μ L of 4% paraformaldehyde for 30 minutes. The cells were then stained in the dark for 30 minutes using a 0.5% crystal violet dye solution (C0121, Beyotime, Shanghai, China). The cells and excess dye solution remaining on the polycarbonate membrane in the upper chamber were removed with cotton swabs, and the chamber was subsequently dried. Cells that penetrated the polycarbonate membrane were imaged using a Zeiss inverted microscope, and their number quantified using Image J software.

Transwell invasion assay. Before the experiment, RPMI 1640 culture medium was mixed with Matrigel matrix glue (354234, Corning, Steuben County, New York, USA) in a 1:7 volume ratio. Subsequently, 60 μ L of this mixture was placed in the upper chamber of the Transwell and left to incubate overnight. The remaining experimental procedures were the same as those used in the cell migration assay.

2.12 RNA-Pull Down and Mass-Spectrometry Assay

A total of 400 μ L of HTR-8/SVneo cellular protein solution was divided equally into 4 groups (Sense, Anti-sense, Input and Beads). Biotin-labeled tiRNA-Gln-CTG and its control probe were incubated with cytoplasmic protein solution at 4 °C overnight (no probe was added to the beads group) to form RNA-protein complexes. Agarose beads (30 μ L) were added to three 1.5 mL enzyme-free EP tubes (151440, MedChemExpress, Monmouth Junction, NJ, USA) and centrifuged for 30 seconds. The upper liquid layer was discarded and the beads were resuspended in 200 μ L of PBS and centrifuged at room temperature (3000 g, 1 minute). The supernatant was discarded and the procedure was repeated five times. The RNA-protein complexes were then combined with the agarose beads and incubated at 4 °C for 1 h with rotation. Following centrifugation (3000 g, 1 minute), the supernatant was discarded and the pellet was resuspended in 200 μ L of PBS. This step was repeated nine times. Finally, after adding 40 μ L of SDS-PAGE sample buffer and incubating in a 100 °C water bath for 10 minutes, the samples underwent 10% SDS-PAGE electrophoresis followed by rapid silver staining (P0017S, Beyotime, Shanghai, China).

The SDS gel was cut into 1 mm pellets with a scalpel and placed into 2 mL centrifuge tubes. Decolorizing solu-

tion (25 mM ammonium bicarbonate and acetonitrile) was added and the tubes were evenly shaken. This was repeated several times until the destaining was complete. Ethyl ether was added to dehydrate the pellet until it turned white, followed by vacuum drying. Dithiothreitol (10 mM, D9779, Sigma-Aldrich, St. Louis, MO, USA) was then added and incubated for 60 min at 56 °C. An iodoacetamide solution (55 mM, RPN6302, GE Healthcare, Chicago, IL, USA) was added and reacted for 45 min in the dark. A trypsin solution (10 ng/ μ L, V5111, Promega, Madison, WI, USA) was then added to fully cover the pellet and left at 37 °C overnight. The next day, the extraction solution (50% acetonitrile + 3% trifluoroacetic acid) and 100% acetonitrile were added and the sample centrifuged. The resulting supernatant with enzyme solution was collected in a new centrifuge tube, vacuum dried and then stored at -20 °C. Peptides were analyzed via elution using an EASY-nLC 1200 UHPLC system (EASY-nLC 1200, Thermo Fisher Scientific, Waltham, MA, USA), and using a Thermo Q Exactive HF-X mass spectrometer (Q Exactive HF-X, Thermo Fisher Scientific, Waltham, MA, USA) following elution and ionization.

2.13 Dual-Luciferase-Reporter Assay

The 3'UTR of the *THBS2* sequence containing the tiRNA-Gln-CTG binding site was inserted into the SacI/XhoI restriction site of the pmirGLO vector (GenePharma, Shanghai, China). It contained either a wild-type (WT) or mutant (MUT) sequence. HEK293T cells were transfected with a luciferase-reporter vector and either a tiRNA-Gln-CTG mimic or control using Lipofectamine 3000. After transfection for 48 h, firefly and renilla luciferase activities were measured using a luciferase assay system (Glomax 96, Promega, Madison, WI, USA) as per the manufacturer's guidelines (G1701, Servicebio, Wuhan, Hubei, China).

2.14 WB Assay

HTR-8/SVneo cells underwent two PBS washes before the addition of 60 μ L of a radioimmunoprecipitation (RIPA) assay lysate mixture containing phenylmethanesulfonyl fluoride and a protease inhibitor (all from Beyotime, Shanghai, China). The cells were thoroughly lysed on ice and the protein concentration was then measured with a BCA protein assay kit (P0012, Beyotime, China). Although 20 μ g of protein is typically utilized for WB experiments, we loaded 5–10 μ g of extracellular vesicle (EV)-derived protein for exosome identification, and 10 μ g for cell-derived proteins. The sample volume used for the EV-free group was 15 μ L. The ratio of cell supernatant without EVs to loading buffer was 4:1. Following separation by 10% polyacrylamide gel electrophoresis, proteins were transferred to a polyvinylidene fluoride membrane. After blocking with 5% skim milk or bovine serum albumin for 2 h, membranes were incubated overnight on a shaker with primary antibody. They were then washed three

times for 10 minutes each with Tris Buffered Saline containing Tween-20 (TBST) on a shaker, followed by incubation with the secondary antibody for 1 h at room temperature. After three washes with TBST, protein bands were visualized with a chemiluminescent reagent (WBKLS0500, Darmstadt, Germany). Image J software was used to semi-quantify the grayscale values of the immunoblots. Information on the antibodies used in WB is presented in **Supplementary File 1**.

2.15 Isolation and Identification of HTR-8/SVneo Cell-Derived EVs

HTR-8/SVneo cells were incubated for 36 h in a medium containing EV-free FBS (C380109199, VivaCell Bioscience, Shanghai, China). The medium was then collected and EVs were isolated using the VEX Exosome Isolation Reagent (R601, Vazyme, Nanjing, Jiangsu, China) as per the manufacturer's instructions. Cell culture medium was filtered through a 0.22 μ M pore filter to remove cell debris, followed by centrifugation at 5600 rpm for 20 minutes at 4 °C. Subsequently, Exosome Isolation Reagent was added to the supernatant at a 1:3 ratio and mixed thoroughly. After refrigerating for 16 h at 4 °C, the supernatant was removed after centrifugation (10200 rpm, 30 minutes, 4 °C) and the pellet resuspended in PBS to obtain the exosome suspension. The size and shape of EVs were observed using transmission electron microscopy (HT7800, Hitachi, Chiyoda-ku, Tokyo, Japan), and the expression of cluster of differentiation 63 (CD63), cluster of differentiation 81 (CD81), ALG-2-interacting protein X/apoptosis-linked gene 2-interacting protein 1 (ALIX), tumor susceptibility gene 101 (TSG101), heat shock protein 70 (HSP70) and golgi matrix protein 130 (GM130) proteins was evaluated by WB assay.

2.16 Fluorescent In Situ Hybridization (FISH) Assay

HTR-8/SVneo cells were cultured in 24-well plates with cell coverslips. They were then fixed in 4% formaldehyde and permeabilized with 0.5% Triton X-100. A FAM-labeled tiRNA-Gln-CTG probe was designed and synthesized by GenePharma (Shanghai, China). The FISH assay was performed as recommended by the reagent supplier (C10910, RiboBio, China). A suitable field of view was chosen and imaged using a Zeiss fluorescence microscope (Oberkochen, Germany) to examine the localization of tiRNA-Gln-CTG in HTR-8/SVneo cells.

2.17 Statistical Analysis

Data analysis was conducted using SPSS (Version 20.0, International Business Machines Corporation, Armonk, New York, USA) and GraphPad Prism (Version 8.0, GraphPad software, San Diego, CA, USA). Study results were expressed as the mean \pm standard deviation (SD). Statistical significance between two data groups was determined using a two-tailed Student's *t*-test. One-way

ANOVA followed by Tukey's post hoc test was used for comparisons among multiple data groups. The Shapiro-Wilk test evaluated the normality of tsRNA level distributions in plasma, as well as the baseline characteristics of women with suspected PE. Normal distributions were analyzed using the unpaired Student's *t*-test. Non-normal distributions were assessed with the Mann-Whitney U test, with data presented as the median and interquartile range. A *p*-value of 0.05 or lower was considered statistically significant. Individual *p*-values were noted when appropriate. The predictive diagnostic efficacy of serum tiRNA-Gln-CTG for suspected PE cases was evaluated using a receiver operating characteristic (ROC) curve and the area under the curve (AUC). Each experiment was conducted independently a minimum of three times. The data of qRT-PCR, EdU, wound healing, transwell and WB experiments were all presented after normalization. The level of tiRNA in the plasma of patients with suspected PE was presented in the form of Δ CT.

3. Results

3.1 tsRNA Expression in the Plasma of Patients with PE Compared to Healthy Pregnant Controls

High-throughput sequencing of tsRNA was performed to compare the level of tsRNA in plasma from PE and healthy control women (Fig. 1A). Different subclasses of tsRNAs were distributed according to their size and length (Fig. 1B,C). Results above indicated that significant differences existed in the composition of the tsRNA profile and the expression level of tsRNA between the PE and healthy control groups. Identifying the differential tsRNAs is the primary step for their roles in the development of PE and their potential as predictive markers for PE. A total of 1532 tsRNAs showed elevated counts per million (CPM) mapped read values of >1.5 -fold in the PE plasma compared to healthy controls, while 814 showed decreased values (Fig. 1D). Of these, 28 were significantly up-regulated (unadjusted *p* < 0.05), while 59 were significantly down-regulated (Fig. 1E). Fig. 1F shows the categorization of the differential tsRNAs.

3.2 Expression of tiRNA-Gln-CTG in the Plasma and Placenta of PE Women, and Exploration of Potential Biological Functions

tsRNAs with CPM >1.5 and *p* < 0.05 were selected for potential biological function analysis using the TargetScan, miRanda, and Metascape bioinformatics tools. Ultimately, 6 tsRNAs were chosen for further experiments based on GO and KEGG analysis results suggesting they were potentially involved in the development of PE (Fig. 2A). These tsRNAs were subsequently analyzed in the placenta and plasma samples of both PE patients and healthy controls. The expression levels of the 6 tsRNAs in plasma aligned closely with the high-throughput sequencing results (Fig. 2B). High-throughput tRF and tiRNA

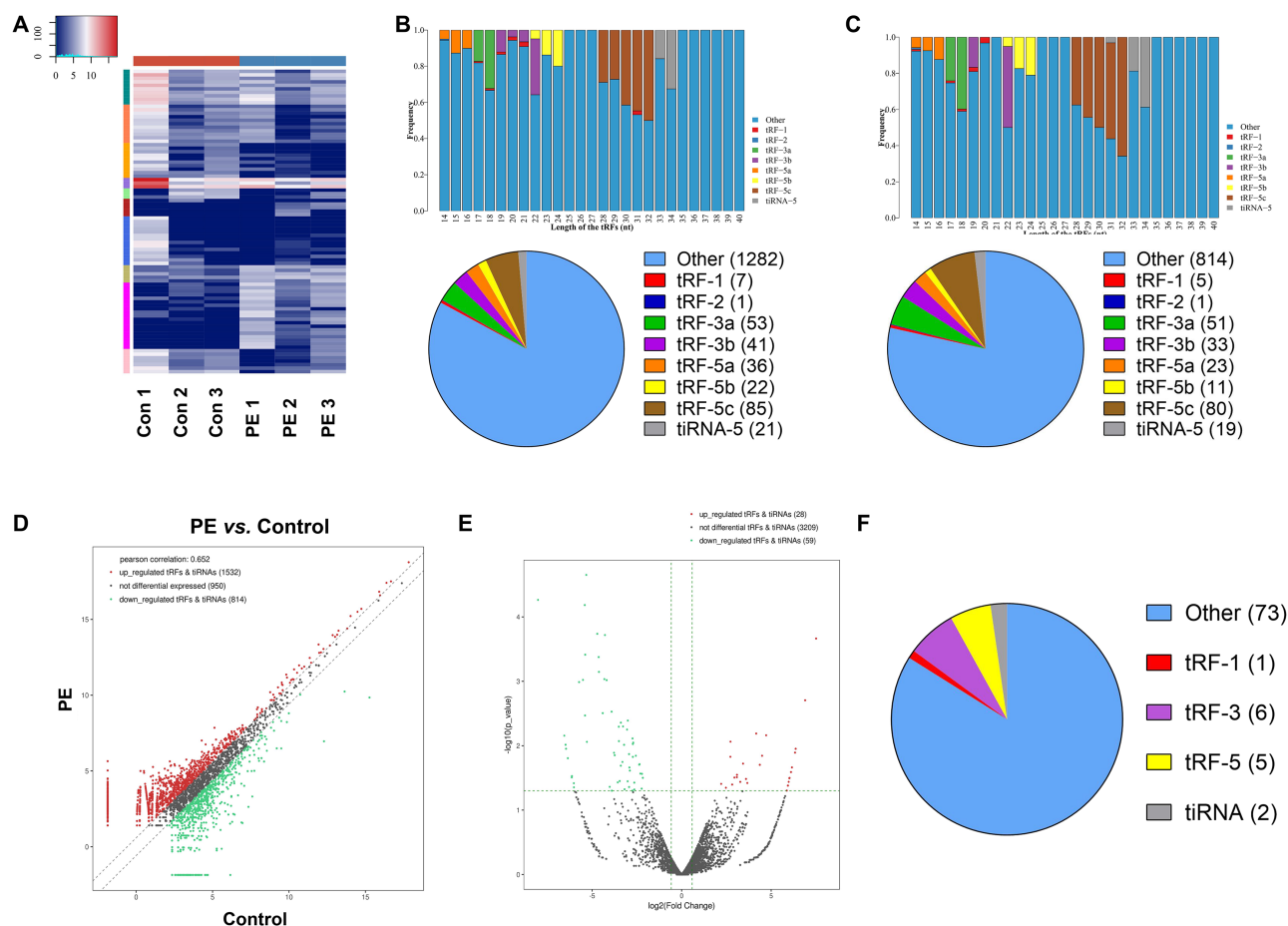


Fig. 1. Expression profiles of tsRNA in the plasma of pregnant women with PE ($n = 3$) and healthy pregnant women ($n = 3$). (A) Heat map of differential tsRNAs. (B) Distribution of tsRNA species in the plasma of healthy pregnant women. (C) Distribution of tsRNA species in the plasma of women with PE. (D) tsRNAs with >1.5-fold differential expression. (E) Volcano plot of differential tsRNAs. (F) Categorization of the differential tsRNAs. PE, pre-eclampsia; tsRNA, transfer ribonucleic acid-derived small RNA; tiRNA, transfer ribonucleic acid halves; tRF, transfer ribonucleic acid-derived fragment.

sequencing revealed that tRF-SeC-TCA expression levels were significantly lower in the plasma of patients with PE compared to healthy controls. The plasma verification results showed that the levels of tRF-SeC-TCA in patients with PE did not decrease significantly. The expression of three of these tsRNAs (tRF-Ser-TGA, tiRNA-Gln-CTG and tRF-Cys-GCA) in the placenta was consistent with that found in plasma (Fig. 2C). tiRNA-Gln-CTG was chosen for further analysis in subsequent experiments because the biological process of its possible 3'UTR mRNA binding targets were involved in the cellular response to oxidative stress, cell migration, and cell proliferation (Fig. 3A). Oxidative stress and altered cellular functions in the placenta are key factors in the pathogenesis of PE. Moreover, the cellular component involved the cell leading edge, cell body, and perinuclear region of cytoplasm (Fig. 3B). The molecular function included salt transmembrane-transporter activity, while protein molecular function encompassed salt transmembrane transporter

activity, protein serine/threonine kinase activity, and acyl-transferase activity (Fig. 3C). KEGG pathway analysis also indicated that tiRNA-Gln-CTG may play a role in classical signaling pathways, including mitogen-activated protein kinase (MAPK), forkhead box, sub-group O (FoxO), and phosphatidylinositol 3-kinase/protein kinase B (PI3K-AKT, Fig. 3D). Protein-protein interaction (PPI) network maps were drawn to analyze the potential core target genes of tiRNA-Gln-CTG (Fig. 3E). The structure of tiRNA-Gln-CTG is shown in Fig. 3F.

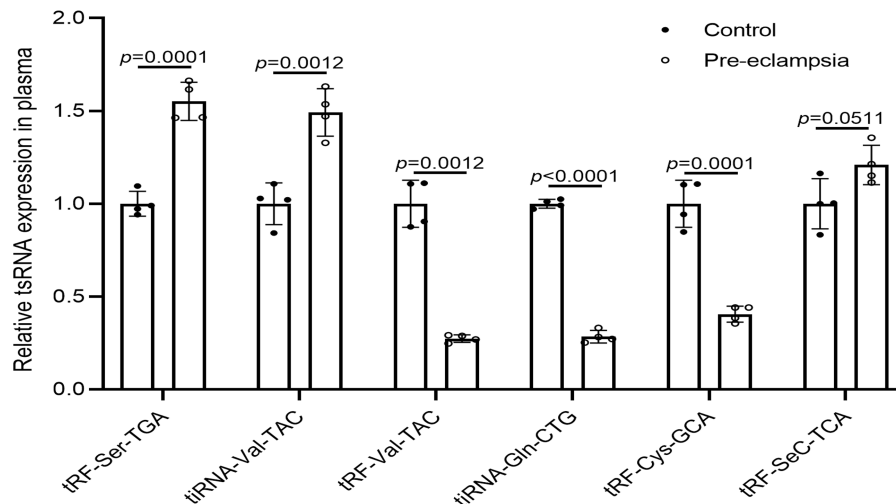
3.3 Intracellular Localization of tiRNA-Gln-CTG, and its Expression and EV-Mediated Secretion in Hypoxia-Induced HTR-8/SVneo Cells

FISH experiments revealed that tiRNA-Gln-CTG was expressed in both the cytoplasm and nucleus of HTR-8/SVneo cells (Fig. 4A). Hypoxia models of HTR-8/SVneo cells were created using varying CoCl_2 concentrations to mimic the placental hypoxic conditions in PE [26–28]. The expression level of HIF-1 α in the cells was evaluated, lead-

A

tsRNA_ID	tsRNA_Seq	log ₂ FC	p
tRF-Ser-TGA	GCAGCGATGGCCGAGTGGTTAAGG	4.363	0.020
tiRNA-Val-TAC	GGTTCATAGTGTAGCGTTATCACGTCTGCTTT	2.720	0.015
tRF-Val-TAC	GCCCCAGTGAACCACCA	-3.051	0.006
tiRNA-Gln-CTG	GGTTCATGGTGTAATGGTTAGCACTCTGGACTC	-3.073	0.022
tRF-Cys-GCA	ATCCAGGTGCCCCCTCCA	-3.189	0.047
tRF-SeC-TCA	GCCCGGATGATCCTC	-3.570	0.037

B



C

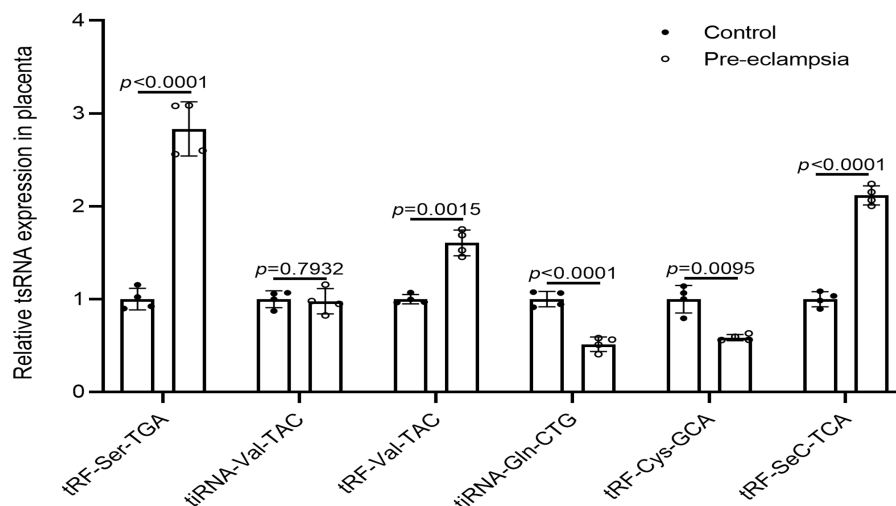


Fig. 2. Expression levels of 6 selected tsRNAs in the plasma and placenta of women with pre-eclampsia and healthy pregnant controls. Data are presented as the mean \pm SD. (A) Basic information about the 6 tsRNAs. (B) Expression levels in plasma for the PE and control groups. (C) Expression levels in placenta for the two groups.

ing to the selection of 100 μ M CoCl₂ for subsequent experiments (Fig. 4B). The concentration of CoCl₂ used previously in the literature ranges mainly from 50 to 250 μ M. Our experiments revealed that concentrations between 50–250 μ M significantly increased the HIF-1 α protein level.

However, HTR-8/SVneo cells underwent significant apoptosis when the CoCl₂ concentration exceeded 100 μ M, as observed under the microscope. Therefore, the concentration of 100 μ M was selected for subsequent experiments. EVs were isolated from the cell culture medium

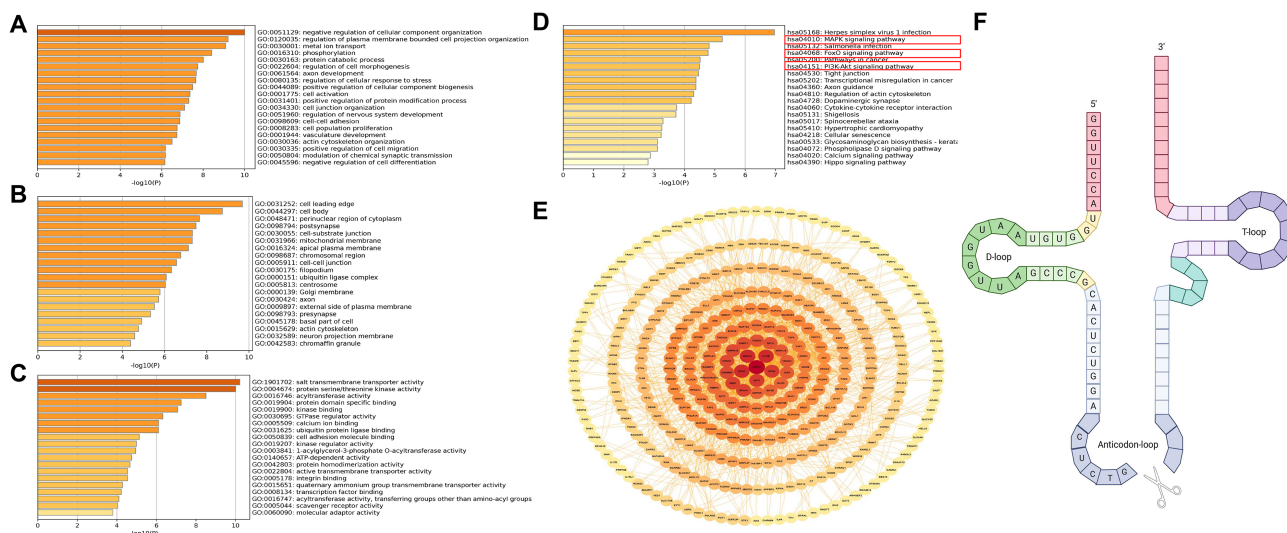


Fig. 3. Analysis of the potential biological functions of tiRNA-Gln-CTG. (A) Biological process categories. (B) Cellular component categories. (C) Molecular function categories. (D) Canonical signaling pathways. (E) PPI network analysis. (F) Structure of tiRNA-Gln-CTG. PPI, protein-protein interaction.

and their structure analyzed by transmission electron microscopy (Fig. 4C). The expression of EV signature proteins was also detected using WB (Fig. 4D). Following CoCl₂-induced hypoxia, the expression of tiRNA-Gln-CTG was significantly reduced in HTR-8/SVneo cells, in the cell culture medium, and in EVs present in the culture medium (Fig. 4E–G).

3.4 Role of tiRNA-Gln-CTG in Modulating HTR-8/SVneo Cell Proliferation, Cell Cycle, Migration, and Invasion

Transfection with the tiRNA-Gln-CTG inhibitor did not significantly alter the expression of tiRNA-Gln-CTG in HTR-8/SVneo cells compared to the control group (Fig. 5A). However, the cell viability (Fig. 5B), proliferation (Fig. 5C), wound healing (Fig. 5D), and cell migration and invasion (Fig. 5E) were all significantly reduced 48 h after transfection with the inhibitor. Moreover, cells transfected with the tiRNA-Gln-CTG inhibitor exhibited a lower proportion of cells in the S-phase, and a significantly higher proportion in the G0/G1 phase (Fig. 5F). No significant difference in the apoptosis level (Fig. 5G) was observed between the two groups.

Transfection with the tiRNA-Gln-CTG mimic led to a significant 55-fold increase in tiRNA-Gln-CTG expression in HTR-8/SVneo cells (Fig. 6A). Cell viability (Fig. 6B), cell proliferation (Fig. 6C), wound healing (Fig. 6D), and cell migration and invasion (Fig. 6E) were all significantly increased 48 h after transfection with the tiRNA-Gln-CTG mimic. The mimic group also exhibited a significantly higher proportion of cells in the S-phase, and a reduced proportion in the G0/G1 phase compared to the mimic-NC group (Fig. 6F). No significant difference in the apoptosis level was observed between the two groups (Fig. 6G).

3.5 tiRNA-Gln-CTG Regulates HTR-8/SVneo Cell Function by Targeting the THBS2 mRNA 3'UTR Region, Leading to its Degradation

The TargetScan and miRanda websites predicted that tiRNA-Gln-CTG binds to the THBS2 mRNA 3'UTR region as 8mer-1u (Fig. 7A). The 3'UTR of THBS2 containing WT or MUT sequence for the tiRNA-Gln-CTG binding site was inserted into the SacI/XhoI restriction site of the pmirGLO Dual-Luciferase miRNA Target Expression Vector (Fig. 7B). Dual luciferase assay showed the relative fluorescence intensity was elevated when HEK293T cells were simultaneously transfected with tiRNA-Gln-CTG inhibitor and GP-miRGLO-THBS2-WT, whereas the relative fluorescence intensity was significantly decreased when they were simultaneously transfected with tiRNA-Gln-CTG mimic and GP-miRGLO-THBS2-WT (Fig. 7C). Transfection of HTR-8/SVneo cells with a tiRNA-Gln-CTG inhibitor significantly increased THBS2 mRNA and protein levels, while transfection with a tiRNA-Gln-CTG mimic significantly reduced these levels (Fig. 7D,E). Moreover, THBS2 protein expression was significantly higher in PE placentas (Fig. 7F), and the THBS2 protein level was also significantly increased in CoCl₂-induced HTR-8/SVneo cells (Fig. 7G). These findings indicate that THBS2 significantly influences the biological functions of tiRNA-Gln-CTG.

Co-transfection of HTR-8/SVneo cells with a tiRNA-Gln-CTG inhibitor and THBS2-siRNA significantly reduced THBS2 mRNA (Fig. 8A) and protein (Fig. 8B) expression levels in the cells. Reduction of THBS2 expression improved the viability (Fig. 8C), proliferation (Fig. 8D), wound healing (Fig. 8E), and migratory and invasive abilities (Fig. 8F). Reduced THBS2 expression also lowered the

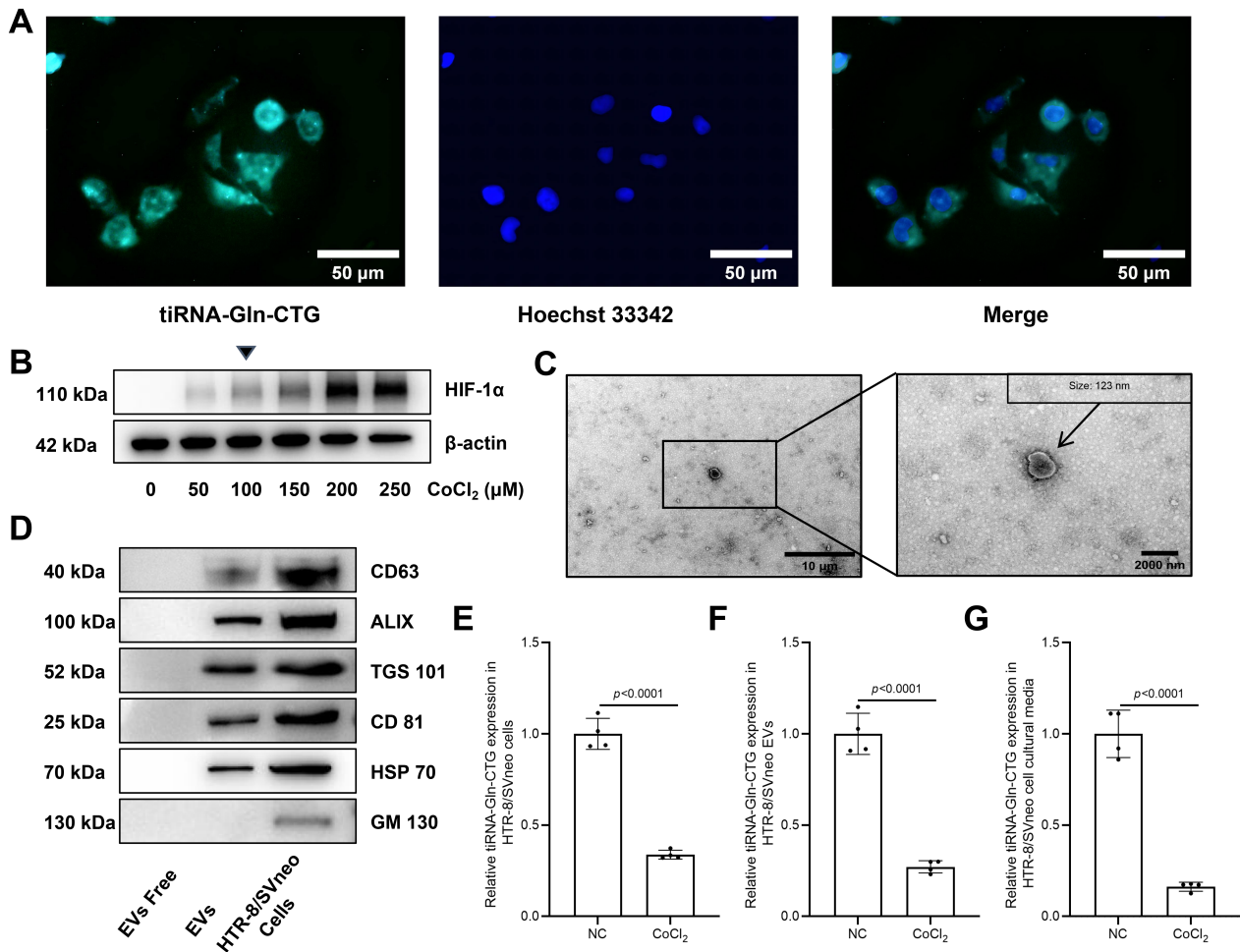


Fig. 4. Localization of tiRNA-Gln-CTG in HTR-8/SVneo cells, and its expression and secretion in a CoCl₂-induced HTR-8/SVneo cell model of PE. Data are presented as the mean \pm SD. (A) Localization of tiRNA-Gln-CTG in HTR-8/SVneo cells (scale bar = 50 μ m). (B) HIF-1 α expression levels in the PE trophoblast cell model under different concentrations of CoCl₂. For subsequent experiments, 100 μ M CoCl₂ was selected to induce hypoxia. (C) Transmission electron microscopy showing the morphology of EVs extracted from HTR-8/SVneo cell culture medium (scale bar = 10 μ m, left; scale bar = 2000 nm, right). (D) Western blot identification of the signature proteins for EVs. (E) Expression level of tiRNA-Gln-CTG in HTR-8/SVneo cells from the PE trophoblast cell model, $n = 4$ per group. (F) Expression level of tiRNA-Gln-CTG in EVs from the culture medium of the PE trophoblast cell model, $n = 4$ per group. (G) Expression level of tiRNA-Gln-CTG in culture medium from the PE trophoblast cell model, $n = 4$ per group. EV, extracellular vesicle; NC, normal control; CD63, cluster of differentiation 63; CD81, cluster of differentiation 81; ALIX, ALG-2-interacting protein X/apoptosis-linked gene 2-interacting protein 1; TGS101, tumor susceptibility gene 101; HSP70, heat shock protein 70; GM130, golgi matrix protein 130. NC, negative control.

proportion of cells in the G0/G1 phase, while increasing the proportion in the proliferative phase (Fig. 8G), however the apoptosis level remained unchanged (Fig. 8H).

3.6 tiRNA-Gln-CTG may Regulate the Expression of Multiple Proteins Related to its Biological Functions by Affecting AKT Phosphorylation

tiRNA-Gln-CTG sense and antisense molecules were identified by nucleic acid electrophoresis (Fig. 9A). RNA pull-down assay (Fig. 9B) and mass spectrometry revealed that tiRNA-Gln-CTG could specifically bind to 45 proteins

(Fig. 9C). YBX1 was chosen for further validation due to its involvement in the regulation of gene expression and in non-coding RNA incorporation into the exosome. *In vitro* experiments confirmed that tiRNA-Gln-CTG specifically binds to YBX1 (Fig. 9D). The YBX1 expression level was reduced after transfection of YBX1-siRNA (Fig. 9E). The expression of tiRNA-Gln-CTG in HTR-8/SVneo cells remained unchanged following transfection of YBX1-siRNA (Fig. 9F), but its expression was significantly reduced in EVs present in the culture medium (Fig. 9G), as well as in the culture medium itself (Fig. 9H). AKT occupies a cen-

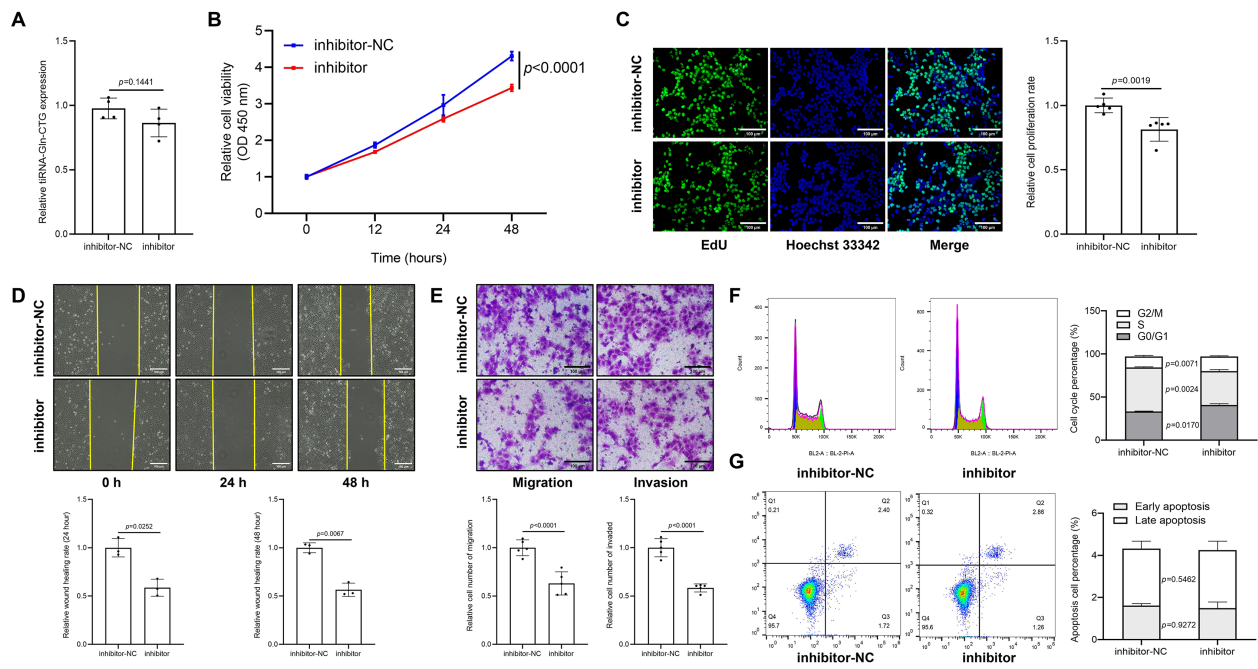


Fig. 5. Effect of transfection with the tiRNA-Gln-CTG inhibitor on HTR-8/SVneo cell function. Data are presented as the mean \pm SD. (A) The tiRNA-Gln-CTG level after transfection with tiRNA-Gln-CTG inhibitor, $n = 4$ per group. (B) CCK-8 assay, $n = 6$ per group. (C) EdU assay, $n = 5$ per group (scale bar = 100 μ m). (D) Wound healing assay, $n = 3$ per group (scale bar = 100 μ m). (E) Transwell cell migration and invasion assay, $n = 5$ per group (scale bar = 100 μ m). (F) Cell cycle, $n = 3$ per group. (G) Cell apoptosis, $n = 3$ per group. EdU, 5-ethynyl-2'-deoxyuridine.

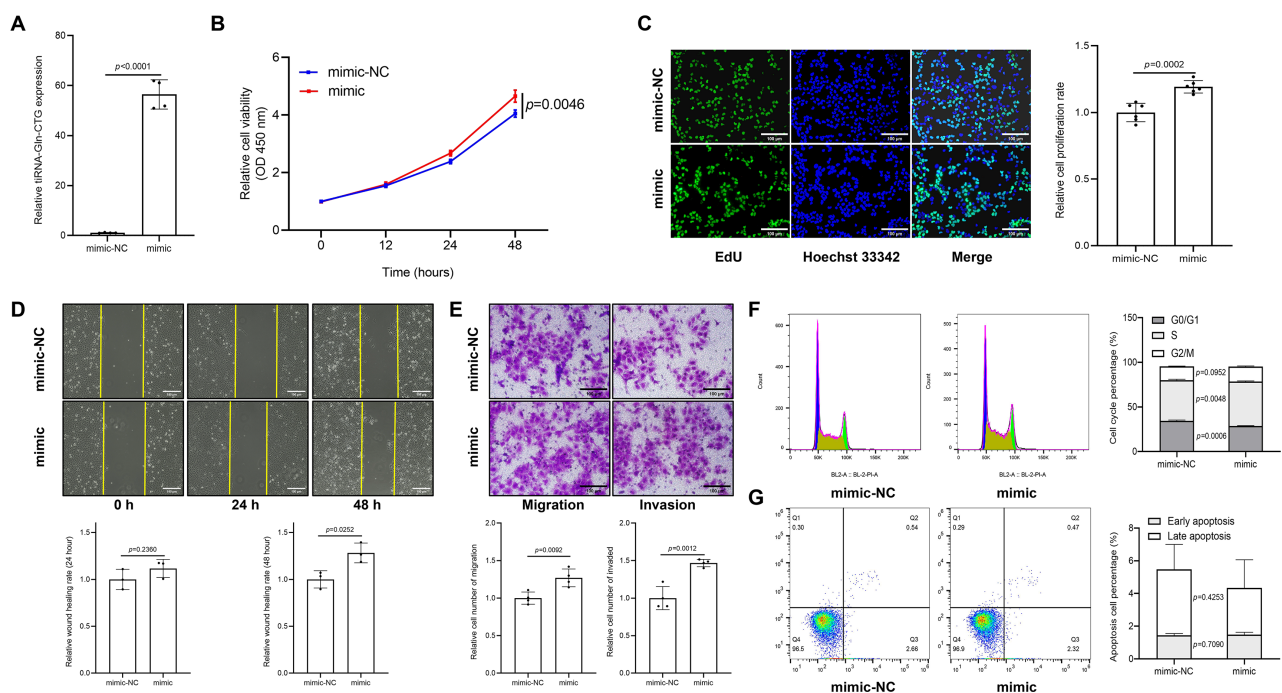


Fig. 6. Effect of transfection with the tiRNA-Gln-CTG mimic on HTR-8/SVneo cell function. Data are presented as the mean \pm SD. (A) The tiRNA-Gln-CTG level after transfection with the tiRNA-Gln-CTG mimic, $n = 4$ per group. (B) CCK-8 assay, $n = 6$ per group. (C) EdU assay, $n = 6$ per group (scale bar = 100 μ m). (D) Wound healing assay, $n = 3$ per group (scale bar = 100 μ m). (E) Transwell cell migration and invasion assay, $n = 5$ per group (scale bar = 100 μ m). (F) Cell cycle, $n = 3$ per group. (G) Cell apoptosis, $n = 3$ per group.

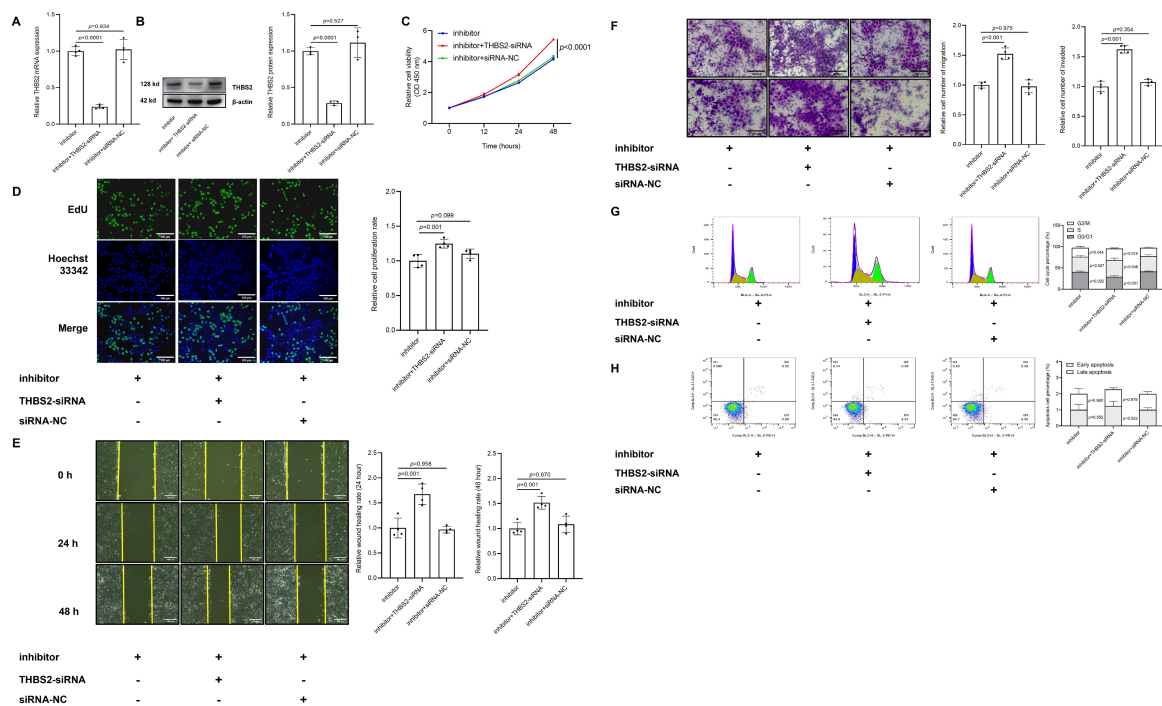


Fig. 8. Cellular functions of HTR-8/SVneo cells after co-transfection with tiRNA-Gln-CTG inhibitor and siRNA-THBS2. Data are presented as the mean \pm SD. (A) *THBS2* mRNA expression level after co-transfection of tiRNA-Gln-CTG inhibitor with siRNA-THBS2, $n = 4$ per group. (B) Western blot detection of THBS2 protein expression after co-transfection of tiRNA-Gln-CTG inhibitor with siRNA-THBS2, $n = 3$ per group. (C) CCK-8 assay, $n = 6$ per group. (D) EdU assay, $n = 4$ per group (scale bar = 100 μ m). (E) Wound healing assay, $n = 4$ per group (scale bar = 100 μ m). (F) Transwell cell migration and invasion assay, $n = 4$ per group (scale bar = 100 μ m). (G) Cell cycle, $n = 3$ per group. (H) Cell apoptosis, $n = 3$ per group.

tral position in the PPI interaction network analysis. The present results suggest that tiRNA-Gln-CTG exerts its biological function possibly through its regulation of AKT phosphorylation (Fig. 9I). This study also identified several signature proteins associated with the biological function of tiRNA-Gln-CTG, notably changes in the expression levels of cyclin D1, proliferating cell nuclear antigen (PCNA), vimentin, N-cadherin, and E-cadherin, whereas the expression levels of B-cell lymphoma/leukemia-2 (Bcl2) and Bcl-2 associated X (Bax) remained unchanged (Fig. 9J,K).

3.7 tiRNA-Gln-CTG is a Powerful Biomarker for Predicting Suspected Cases of PE

A total of 122 women with a suspected diagnosis of PE were enrolled in the study (Table 1), of whom 28 ultimately developed PE and 94 did not (non-PE group). Women who developed PE had a lower body mass index (BMI) ($p = 0.036$), delivered earlier ($p < 0.001$), and were more likely to have a cesarean delivery ($p < 0.001$) than the non-PE group. Women who were suspected of having PE due to elevated blood pressure had a higher proportion of ultimately developing PE ($p = 0.002$). In this study of 122 patients with suspected PE, plasma tiRNA-Gln-CTG levels were used to predict the likelihood of developing PE within the following week (Fig. 10A), the following 4 weeks (Fig. 10B), and

before the termination of pregnancy (Fig. 10C). The sensitivity of reduced tiRNA-Gln-CTG for predicting the onset of PE at these times was 91.7%, 85.7%, and 89.3%, respectively, while the specificity was 84.5%, 79.2%, and 73.4% (Fig. 10D).

4. Discussion

Certain 5'tiRNAs, including a group of tRF-3a, are notably upregulated at the maternal-fetal interface during immune activation in mice [16]. 5'-tRFs are the primary small RNA species secreted by pre-eclamptic syncytiotrophoblasts [29]. Oxidative stress regulates tiRNA production [30], and both hypoxia and oxidative stress are key mechanisms in placental PE [31]. The investigation of changes in tsRNA expression and their functions in PE could provide novel insights for the prediction and treatment of this condition. The present study is the first to report the use of plasma tiRNA-Gln-CTG to predict the future occurrence of PE in women who are suspected of having this condition.

A lower plasma tiRNA-Gln-CTG level was found to be a biomarker for predicting the onset of PE within one week in women suspected of being at risk for this condition. CoCl₂ induces oxidative stress in trophoblasts, thus prompting its use in a hypoxia model that uses HTR-

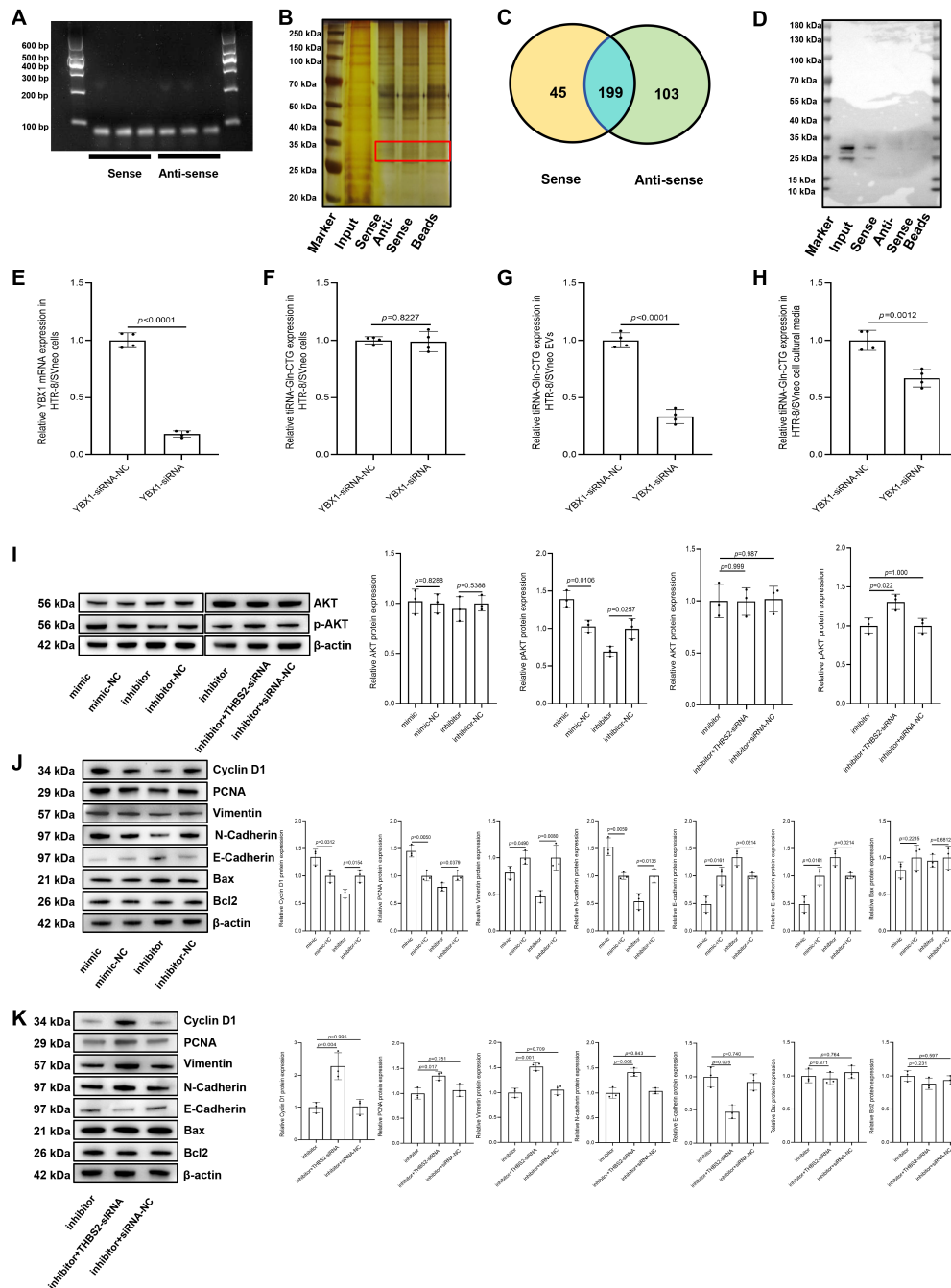


Fig. 9. Preliminary investigation of the mechanism by which tiRNA-Gln-CTG is sorted into EVs and mediates their biological functions. Data are presented as the mean \pm SD. (A) Identification of sense and antisense tiRNA-Gln-CTG, $n = 3$ per group. (B) RNA pull-down assay used to probe the proteins bound to tiRNA-Gln-CTG. (C) Mass spectrometry analysis used to probe differential proteins in sense and antisense tiRNA-Gln-CTG. (D) *In vitro* validation of the binding of tiRNA-Gln-CTG to YBX1. (E) *YBX1* mRNA expression levels after transfection of YBX1-small interfering RNA (siRNA), $n = 4$ per group. (F) tiRNA-Gln-CTG expression level in HTR-8/SVneo cells after YBX1 silencing, $n = 4$ per group. (G) tiRNA-Gln-CTG expression level in EVs secreted by HTR-8/SVneo cells after YBX1 silencing, $n = 4$ per group. (H) tiRNA-Gln-CTG expression level in the HTR-8/SVneo cell culture medium after YBX1 silencing, $n = 4$ per group. (I) tiRNA-Gln-CTG may degrade *THBS2* mRNA and mediate AKT phosphorylation to carry out its biological functions, $n = 3$ per group. (J-K) tiRNA-Gln-CTG has important effects on the expression of some functional proteins that regulate HTR-8/SVneo cells, $n = 3$ per group. YBX1, Y-box-binding protein 1; AKT, protein kinase B.

Table 1. Clinical information on women who developed PE.

	PE (<i>n</i> = 28)	Non-PE (<i>n</i> = 94)	$\chi^2/t/Z$	<i>p</i>
Age (yrs), median (IQR)	33.00 (6.50)	31.50 (6.00)	−1.521	0.128
BMI (kg/m ²), median (IQR)	26.66 (5.99)	29.43 (6.70)	−2.100	0.036
Gestational week at suspected PE (weeks), median (IQR)	33.29 (3.89)	32.29 (3.61)	−0.006	0.995
Gestational week for PE diagnosis (weeks), median (IQR)	36.56 (3.14)	—	—	—
Gestational week of delivery (weeks), median (IQR)	36.93 (1.75)	38.79 (1.61)	−5.486	<0.001
tiRNA-Gln-CTG Δ CT	6.87 \pm 1.18	5.55 \pm 0.94	−6.133	<0.001
Mode of delivery, <i>n</i> (%)				
Vaginal delivery	2 (7.14)	40 (42.55)	11.983	<0.001
Cesarean section	26 (92.86)	54 (57.45)		
Diagnostic indicators of suspected PE, <i>n</i> (%)				
Blood pressure	22 (78.57)	43 (45.74)	9.339	0.002
Abnormal urine protein levels	4 (14.29)	9 (9.57)	0.130	0.719
Elevated aminotransferases	1 (3.57)	20 (21.28)	3.585	0.058
Low platelet	0 (0.00)	2 (2.13)	—	1.000
Suspected IUGR of the fetus	4 (14.29)	31 (32.98)	3.685	0.055

PE, pre-eclampsia; BMI, body mass index; IUGR, intrauterine growth restriction.

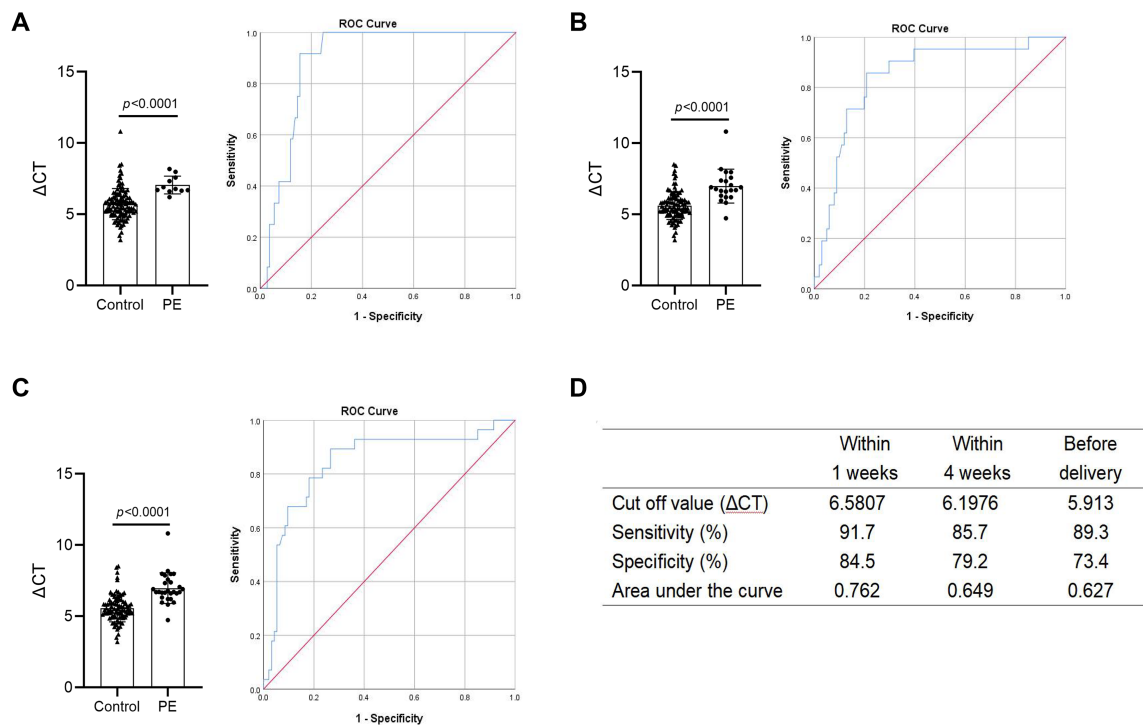


Fig. 10. Receiver operating curves were employed to analyze the predictive ability of plasma tiRNA-Gln-CTG for the future occurrence of PE in women with suspected PE. Data are presented as the mean \pm SD. (A) Predictive efficacy of PE occurring within the next 1 week, $n_{\text{control}} = 110$, $n_{\text{pre-eclampsia}} = 12$. (B) Predictive efficacy of PE occurring within the next 4 weeks, $n_{\text{control}} = 101$, $n_{\text{pre-eclampsia}} = 21$. (C) Predictive efficacy of PE occurring before the termination of pregnancy, $n_{\text{control}} = 94$, $n_{\text{pre-eclampsia}} = 28$. (D) Sensitivity and specificity for the prediction of PE within the next 1 week after suspected diagnosis of PE, within the next 4 weeks, and before delivery.

8/SVneo cells to mimic trophoblast injury in PE. Our findings indicated a significant reduction in the production and secretion of tiRNA-Gln-CTG under conditions of oxidative stress. tiRNA-Gln-CTG plays a role in trophoblast proliferation, migration, invasion, and cell cycle regulation, and its secretion is facilitated by YBX1-mediated EV

encapsulation. Our results suggest that tiRNA-Gln-CTG may function by binding to the 3'UTR of *THBS2* mRNA, thereby facilitating its degradation and subsequently influencing AKT phosphorylation. AKT plays a crucial role in the PI3K/AKT signaling pathway, and its phosphorylation regulates various cellular processes, including growth, sur-

vival, proliferation, and migration [32]. High phosphorylation levels of AKT were found to be associated with protection against oxidative stress in trophoblast cells [33]. In the present study we did not explore the target organs of plasma tsRNA, but rather the function of its regulatory secretory cells. tRF-3022b was reported to be significantly increased in colorectal cancer tissues and plasma exosomes, and tRF-3022b is also involved in regulation of the cell cycle and apoptosis in colorectal cancer cells. This regulation is achieved through secretion of tRF-3022 from the cell, followed by uptake again by the cell [34]. Although tiRNA-Gln-CTG plays a biological role in trophoblasts, we did not examine whether it is directly regulated after production, or whether it is secreted from the cell in EVs and then taken up by trophoblasts to play a regulatory role. Thus, more experiments are needed to validate the mechanism by which tiRNA regulates trophoblast function.

THBS2 is a glycoprotein with diverse biological roles, including angiogenesis, cell motility, apoptosis, and cytoskeletal organization [35,36]. This study demonstrated that THBS2 is negatively regulated by tiRNA-Gln-CTG, as confirmed by bioinformatics analysis and luciferase reporter assays. Additional functional experiments showed that THBS2 knockdown enhanced the effect of a tiRNA-Gln-CTG inhibitor on trophoblast cell proliferation, migration, invasion, and cell cycle progression. Numerous studies have shown that THBS2 is dysregulated in breast, colon, and ovarian cancers, acting as an inhibitor of tumor invasion [37,38]. THBS2 was found to inhibit angiogenesis in endothelial cells through its interaction with matrix metalloproteinases and the extracellular matrix [39]. In the present study, THBS2 protein and mRNA levels were elevated in the placental tissues of PE patients and in the CoCl₂-induced trophoblast-hypoxia model. Taken together, these findings imply that the biological effects of tiRNA-Gln-CTG in trophoblasts may in part be mediated through THBS2.

tRF and tiRNA can influence cell proliferation and the cell cycle by modulating gene expression and interacting with RNA-binding proteins such as YBX1 to inhibit transcription [40]. On the other hand, YBX1 is also involved in exosomal RNA sorting [41]. The entry of some specific RNAs into the exosome requires the sorting action of YBX1 [42]. By exploring the expression and secretion of tiRNA-Gln-CTG after YBX1 silencing, we were able to demonstrate a role for YBX1 in tiRNA sorting.

Thus, our findings demonstrate a role for tiRNA-Gln-CTG in the development of PE, as well as its sorting into EVs. tsRNA is expressed at high abundance in various body fluids and has been considered as a possible biomarker for various diseases [8]. The exploration of tiRNA-Gln-CTG as a candidate biomarker for PE therefore seems to be an important area for future research. In the present study of women with suspected PE during gestation 24⁺⁰–36⁺⁶, lower plasma levels of tiRNA-Gln-CTG were found

to have progressively higher predictive ability for the onset of PE before delivery, up to 4 weeks after the diagnosis of suspected PE, and up to 1 week after the diagnosis of suspected PE. This provides some direction for future studies into diagnostic and predictive indicators of PE. The primary biomarker for predicting PE is the ratio of soluble fms-like tyrosine kinase-1 (sFlt-1) to placental growth factor (PIGF). A cohort study found this indicator has a negative predictive value of 99.3% for predicting PE, with a sensitivity and specificity of 80.0% and 78.3%, respectively [18]. The combined detection of tiRNA-Gln-CTG with this indicator may significantly enhance the sensitivity and specificity of PE diagnosis. Besides tiRNA-Gln-CTG, the KEGG biological functions of tRF-Ser-TGA and tRF-Cys-GCA have revealed associations with signaling pathways including MAPK [43], tumor necrosis factor (TNF) [44], and HIF-1 [45], although they were not further explored in the present study. These signaling pathways contribute to trophoblast cell development in PE. Exploration of the biological roles and molecular mechanisms of various tsRNAs, as well as their potential as biomarkers for predicting PE development in suspected cases, is crucial for optimizing the future management of PE.

An additional point is that tiRNA-Gln-CTG is expressed in both rats and mice [46]. This provides a basis for investigating the effects of placental injection of tiRNA-Gln-CTG on PE symptoms in rat or mouse models. However, the conditions for animal studies are not yet available at our institute and will gradually be carried out in subsequent research programs.

There are several limitations to this study. Firstly, 5'-tRF delivered by circulating EVs was found to reach endothelial cells and macrophages in the vessel wall of pre-eclamptic vessels directly [29]. However, our study did not investigate the effect of EVs on target cells and tissues (mainly endothelial cells and macrophages) after secretion from trophoblasts. Secondly, the RNA pull-down and combined mass-spectrometry analysis did not reveal the traditional Argonaute (AGO) protein family (AGO1, AGO2, AGO3, AGO4) [47]. This of course does not prove that tiRNA-Gln-CTG is unable to form a silencing complex with the AGO proteins. Silencing of the AGO family of genes one by one may be helpful in exploring the role of this family in the biological functions of THBS2. Lastly, our study of the signaling pathways related to the biological functions of THBS2 was not sufficiently thorough and will need further exploration in future research.

5. Conclusions

This is the first study to examine the tsRNA expression profile in the plasma of PE patients and healthy controls. We focused on the role of tiRNA-Gln-CTG in PE development, and its potential as a biomarker for diagnosing suspected cases of PE in pregnant women. We provide new ideas and perspectives for the future diagnosis and treat-

ment of PE. tRNA-Gln-CTG is a potential regulator of trophoblast function during the development of PE. The secretion of tRNA-Gln-CTG into the maternal circulation via EVs is a strong predictive biomarker for the development of PE in women suspected of having this condition.

Availability of Data and Materials

Some of the data used in this study are available from public databases, and the results of high-throughput sequencing of tsRNAs as well as the process of data analysis in this study are available upon request from the corresponding author.

Author Contributions

YXW and XHJ: design of experiments, conduct of experiments, data analysis, and writing of the manuscript. HMS and SCL: design and conduct of experiments, data analysis, and guidance on manuscript revision. HY: design and guidance of experiments, editorial review of the manuscript, and financial support. All authors contributed to editorial changes in the manuscript. All authors contributed to the article and approved the final version. All authors agreed to be accountable for all aspects of the work.

Ethics Approval and Consent to Participate

The Ethics Committee of the Women's Hospital of Nanjing Medical University approved this study (Approval No. 2023KY-003). Except for the database registration, the study adhered to the Declaration of Helsinki standards. All patients enlisted for this research provided written informed consent. They were afforded strict protection of their rights and privacy, and could withdraw from the study at any moment.

Acknowledgment

This is a special acknowledgment. We thank Prof. HJ Ding, Prof. KP Xie, Prof. CB Ji, Prof. XW Cui, Dr. LJ Xu, Dr. CQ Wu, Dr. HY Hou, Dr. Y Yang, Dr. ZY Xia, Dr. L Xue, Dr. ZJ Miao, Miss HY Chen, Miss SY Jiang, Mr. YC Wang, Miss TT Y in and others from Nanjing Medical University. We also thanks Prof. RZ Jia, Dr. X Shen, Dr. SW Feng, Dr. H Yin and others from Zhongda Hospital of Southeast University. The moral and financial support from them helped YX Wang and this research. Thanks to eJear for language editing services on the manuscript.

Funding

This research received no external funding.

Conflict of Interest

The authors declare no conflict of interest.

Supplementary Material

Supplementary material associated with this article can be found, in the online version, at <https://doi.org/10.31083/FBL26345>.

References

- [1] Mirzakhani H, Handy DE, Lu Z, Oppenheimer B, Litonjua AA, Loscalzo J, *et al.* Integration of circulating microRNAs and transcriptome signatures identifies early-pregnancy biomarkers of preeclampsia. *Clinical and Translational Medicine*. 2023; 13: e1446. <https://doi.org/10.1002/ctm2.1446>.
- [2] Jiayu Shen, Xinyuan Teng, Jiayao Zhao, Yuanling Feng, Liquan Wang. A Potential Autophagy-Related-Gene Based Signature in Patients with Preeclampsia. *Frontiers in Bioscience (Landmark Edition)*. 2023; 28: 132. <https://doi.org/10.31083/j.fbl2807132>.
- [3] Chappell LC, Cluver CA, Kingdom J, Tong S. Pre-eclampsia. *Lancet (London, England)*. 2021; 398: 341–354. [https://doi.org/10.1016/S0140-6736\(20\)32335-7](https://doi.org/10.1016/S0140-6736(20)32335-7).
- [4] Ahmed A, Ramma W. Unravelling the theories of pre-eclampsia: are the protective pathways the new paradigm? *British Journal of Pharmacology*. 2015; 172: 1574–1586. <https://doi.org/10.1111/bph.12977>.
- [5] Krishna S, Raghavan S, DasGupta R, Palakodeti D. tRNA-derived fragments (tRFs): establishing their turf in post-transcriptional gene regulation. *Cellular and Molecular Life Sciences*. 2021; 78: 2607–2619. <https://doi.org/10.1007/s00018-020-03720-7>.
- [6] Kumar P, Anaya J, Mudunuri SB, Dutta A. Meta-analysis of tRNA derived RNA fragments reveals that they are evolutionarily conserved and associate with AGO proteins to recognize specific RNA targets. *BMC Biology*. 2014; 12: 78. <https://doi.org/10.1186/s12915-014-0078-0>.
- [7] Zhu P, Yu J, Zhou P. Role of tRNA-derived fragments in cancer: novel diagnostic and therapeutic targets tRFs in cancer. *American Journal of Cancer Research*. 2020; 10: 393–402.
- [8] Shi H, Xie J, Pei S, He D, Hou H, Xu S, *et al.* Digging out the biology properties of tRNA-derived small RNA from black hole. *Frontiers in Genetics*. 2023; 14: 1232325. <https://doi.org/10.3389/fgene.2023.1232325>.
- [9] Jiang P, Yan F. tRNAs & tRFs Biogenesis and Regulation of Diseases: A Review. *Current Medicinal Chemistry*. 2019; 26: 5849–5861. <https://doi.org/10.2174/0929867326666190124123831>.
- [10] Xia L, Guo H, Wu X, Xu Y, Zhao P, Yan B, *et al.* Human circulating small non-coding RNA signature as a non-invasive biomarker in clinical diagnosis of acute myeloid leukaemia. *Theranostics*. 2023; 13: 1289–1301. <https://doi.org/10.7150/thno.80054>.
- [11] Zhang X, Yang P, Khan A, Xu D, Chen S, Zhai J, *et al.* Serum tsRNA as a novel molecular diagnostic biomarker for lupus nephritis. *Clinical and Translational Medicine*. 2022; 12: e830. <https://doi.org/10.1002/ctm2.830>.
- [12] Wang J, Liu X, Cui W, Xie Q, Peng W, Zhang H, *et al.* Plasma tRNA-derived small RNAs signature as a predictive and prognostic biomarker in lung adenocarcinoma. *Cancer Cell International*. 2022; 22: 59. <https://doi.org/10.1186/s12935-022-02481-6>.
- [13] Huang B, Yang H, Cheng X, Wang D, Fu S, Shen W, *et al.* tRF/miR-1280 Suppresses Stem Cell-like Cells and Metastasis in Colorectal Cancer. *Cancer Research*. 2017; 77: 3194–3206. <https://doi.org/10.1158/0008-5472.CAN-16-3146>.
- [14] Cui H, Li H, Wu H, Du F, Xie X, Zeng S, *et al.* A novel 3'tRNA-derived fragment tRF-Val promotes proliferation and inhibits apoptosis by targeting EEF1A1 in gastric cancer. *Cell*

- Death & Disease. 2022; 13: 471. <https://doi.org/10.1038/s41419-022-04930-6>.
- [15] Chen F, Song C, Meng F, Zhu Y, Chen X, Fang X, *et al.* 5'-tRF-GlyGCC promotes breast cancer metastasis by increasing fat mass and obesity-associated protein demethylase activity. *International Journal of Biological Macromolecules*. 2023; 226: 397–409. <https://doi.org/10.1016/j.ijbiomac.2022.11.295>.
 - [16] Su Z, Frost EL, Lammert CR, Przanowska RK, Lukens JR, Dutta A. tRNA-derived fragments and microRNAs in the maternal-fetal interface of a mouse maternal-immune-activation autism model. *RNA Biology*. 2020; 17: 1183–1195. <https://doi.org/10.1080/15476286.2020.1721047>.
 - [17] Yang C, Park S, Song G, Lim W. Inhibition of the cleaved half of tRNA^{Gly} enhances palmitic acid-induced apoptosis in human trophoblasts. *The Journal of Nutritional Biochemistry*. 2022; 99: 108866. <https://doi.org/10.1016/j.jnutbio.2021.108866>.
 - [18] Zeisler H, Llorba E, Chantraine F, Vatish M, Staff AC, Sennström M, *et al.* Predictive Value of the sFlt-1:PIGF Ratio in Women with Suspected Preeclampsia. *The New England Journal of Medicine*. 2016; 374: 13–22. <https://doi.org/10.1056/NEJMoa1414838>.
 - [19] Gestational Hypertension and Preeclampsia: ACOG Practice Bulletin, Number 222. *Obstetrics and Gynecology*. 2020; 135: e237–e260. <https://doi.org/10.1097/AOG.0000000000003891>.
 - [20] Hund M, Allegranza D, Schoedl M, Dilba P, Verhagen-Kamerbeek W, Stepan H. Multicenter prospective clinical study to evaluate the prediction of short-term outcome in pregnant women with suspected preeclampsia (PROGNOSIS): study protocol. *BMC Pregnancy and Childbirth*. 2014; 14: 324. <https://doi.org/10.1186/1471-2393-14-324>.
 - [21] Wang P, Fu Z, Liu Y, Huang S, Guo Y, Jin J, *et al.* tRF-21-LNK8KEP1B as a potential novel diagnostic biomarker for enthesitis-related arthritis. *International Immunopharmacology*. 2023; 124: 110820. <https://doi.org/10.1016/j.intimp.2023.110820>.
 - [22] Jia X, Cao Y, Ye L, Liu X, Huang Y, Yuan X, *et al.* Vitamin D stimulates placental L-type amino acid transporter 1 (LAT1) in preeclampsia. *Scientific Reports*. 2022; 12: 4651. <https://doi.org/10.1038/s41598-022-08641-y>.
 - [23] Zhang C, Ye W, Zhao M, Xia D, Fan Z. tRNA-derived small RNA changes in bone marrow stem cells under hypoxia and osteogenic conduction. *Journal of Oral Rehabilitation*. 2023; 50: 1487–1497. <https://doi.org/10.1111/joor.13566>.
 - [24] Zhou Y, Zhou B, Pache L, Chang M, Khodabakhshi AH, Tanaseichuk O, *et al.* Metascape provides a biologist-oriented resource for the analysis of systems-level datasets. *Nature Communications*. 2019; 10: 1523. <https://doi.org/10.1038/s41467-019-09234-6>.
 - [25] Szklarczyk D, Kirsch R, Koutrouli M, Nastou K, Mehryary F, Hachilif R, *et al.* The STRING database in 2023: protein-protein association networks and functional enrichment analyses for any sequenced genome of interest. *Nucleic Acids Research*. 2023; 51: D638–D646. <https://doi.org/10.1093/nar/gkac1000>.
 - [26] Wang Z, Zhao G, Zibrila AI, Li Y, Liu J, Feng W. Acetylcholine ameliorated hypoxia-induced oxidative stress and apoptosis in trophoblast cells via p38 MAPK/NF-κB pathway. *Molecular Human Reproduction*. 2021; 27: gaab045. <https://doi.org/10.1093/molehr/gaab045>.
 - [27] Xu J, Jia X, Gu Y, Lewis DF, Gu X, Wang Y. Vitamin D Reduces Oxidative Stress-Induced Procaspase-3/ROCK1 Activation and MP Release by Placental Trophoblasts. *The Journal of Clinical Endocrinology and Metabolism*. 2017; 102: 2100–2110. <https://doi.org/10.1210/jc.2016-3753>.
 - [28] Liu J, Yao L, Wang Y. Resveratrol alleviates preeclampsia-like symptoms in rats through a mechanism involving the miR-363-3p/PEDF/VEGF axis. *Microvascular Research*. 2023; 146: 104451. <https://doi.org/10.1016/j.mvr.2022.104451>.
 - [29] Cooke WR, Jiang P, Ji L, Bai J, Jones GD, Lo YMD, *et al.* Differential 5'-tRNA Fragment Expression in Circulating Preeclampsia Syncytiotrophoblast Vesicles Drives Macrophage Inflammation. *Hypertension (Dallas, Tex.: 1979)*. 2024; 81: 876–886. <https://doi.org/10.1161/HYPERTENSIONAHA.123.22292>.
 - [30] Xie Y, Yao L, Yu X, Ruan Y, Li Z, Guo J. Action mechanisms and research methods of tRNA-derived small RNAs. *Signal Transduction and Targeted Therapy*. 2020; 5: 109. <https://doi.org/10.1038/s41392-020-00217-4>.
 - [31] Deer E, Herroek O, Campbell N, Cornelius D, Fitzgerald S, Amaral LM, *et al.* The role of immune cells and mediators in preeclampsia. *Nature Reviews. Nephrology*. 2023; 19: 257–270. <https://doi.org/10.1038/s41581-022-00670-0>.
 - [32] Safdari Y, Khalili M, Ebrahimzadeh MA, Yazdani Y, Farajnia S. Natural inhibitors of PI3K/AKT signaling in breast cancer: emphasis on newly-discovered molecular mechanisms of action. *Pharmacological Research*. 2015; 93: 1–10. <https://doi.org/10.1016/j.phrs.2014.12.004>.
 - [33] Ye L, Huang Y, Liu X, Zhang X, Cao Y, Kong X, *et al.* Apelin/APJ system protects placental trophoblasts from hypoxia-induced oxidative stress through activating PI3K/Akt signaling pathway in preeclampsia. *Free Radical Biology & Medicine*. 2023; 208: 759–770. <https://doi.org/10.1016/j.freeradbiomed.2023.09.030>.
 - [34] Lu S, Wei X, Tao L, Dong D, Hu W, Zhang Q, *et al.* A novel tRNA-derived fragment tRF-3022b modulates cell apoptosis and M2 macrophage polarization via binding to cytokines in colorectal cancer. *Journal of Hematology & Oncology*. 2022; 15: 176. <https://doi.org/10.1186/s13045-022-01388-z>.
 - [35] Yang Y, Li H, Ma Y, Zhu X, Zhang S, Li J. MiR-221-3p is down-regulated in preeclampsia and affects trophoblast growth, invasion and migration partly via targeting thrombospondin 2. *Biomedicine & Pharmacotherapy = Biomedecine & Pharmacotherapie*. 2019; 109: 127–134. <https://doi.org/10.1016/j.biopha.2018.10.009>.
 - [36] Wang X, Zhang L, Li H, Sun W, Zhang H, Lai M. THBS2 is a Potential Prognostic Biomarker in Colorectal Cancer. *Scientific Reports*. 2016; 6: 33366. <https://doi.org/10.1038/srep33366>.
 - [37] Chen J, Yao D, Zhao S, He C, Ding N, Li L, *et al.* MiR-1246 promotes SiHa cervical cancer cell proliferation, invasion, and migration through suppression of its target gene thrombospondin 2. *Archives of Gynecology and Obstetrics*. 2014; 290: 725–732. <https://doi.org/10.1007/s00404-014-3260-2>.
 - [38] Koch M, Hussein F, Woeste A, Gründker C, Frontzek K, Emons G, *et al.* CD36-mediated activation of endothelial cell apoptosis by an N-terminal recombinant fragment of thrombospondin-2 inhibits breast cancer growth and metastasis in vivo. *Breast Cancer Research and Treatment*. 2011; 128: 337–346. <https://doi.org/10.1007/s10549-010-1085-7>.
 - [39] Rödder S, Scherer A, Kömer M, Eisenberger U, Hertig A, Raulf F, *et al.* Meta-analyses qualify metzincins and related genes as acute rejection markers in renal transplant patients. *American Journal of Transplantation: Official Journal of the American Society of Transplantation and the American Society of Transplant Surgeons*. 2010; 10: 286–297. <https://doi.org/10.1111/j.1600-6143.2009.02928.x>.
 - [40] Wang BG, Yan LR, Xu Q, Zhong XP. The role of Transfer RNA-Derived Small RNAs (tsRNAs) in Digestive System Tumors. *Journal of Cancer*. 2020; 11: 7237–7245. <https://doi.org/10.7150/jca.46055>.
 - [41] Suresh PS, Thankachan S, Venkatesh T. Landscape of Clinically Relevant Exosomal tRNA-Derived Non-coding RNAs. *Molecular Biotechnology*. 2023; 65: 300–310. <https://doi.org/10.1007/s12033-022-00546-5>.

- [42] Shurtleff MJ, Yao J, Qin Y, Nottingham RM, Temoche-Diaz MM, Schekman R, *et al.* Broad role for YBX1 in defining the small noncoding RNA composition of exosomes. *Proceedings of the National Academy of Sciences of the United States of America*. 2017; 114: E8987–E8995. <https://doi.org/10.1073/pnas.1712108114>.
- [43] Wang Y, Cheng K, Zhou W, Liu H, Yang T, Hou P, *et al.* miR-141-5p regulate ATF2 via effecting MAPK1/ERK2 signaling to promote preeclampsia. *Biomedicine & Pharmacotherapy = Biomedecine & Pharmacotherapie*. 2019; 115: 108953. <https://doi.org/10.1016/j.biopha.2019.108953>.
- [44] Mohammadpour-Gharehbagh A, Jahantigh D, Eskandari M, Eskandari F, Rezaei M, Zeynali-Moghaddam S, *et al.* The role of TNF- α and TLR4 polymorphisms in the placenta of pregnant women complicated by preeclampsia and in silico analysis. *International Journal of Biological Macromolecules*. 2019; 134: 1205–1215. <https://doi.org/10.1016/j.ijbiomac.2019.05.040>.
- [45] Liu W, Wang SJ, Lin QD. Study on the expressions of PHD and HIF in placentas from normal pregnant women and patients with preeclampsia. *International Journal of Biological Sciences*. 2014; 10: 278–284. <https://doi.org/10.7150/ijbs.6375>.
- [46] Zuo Y, Zhu L, Guo Z, Liu W, Zhang J, Zeng Z, *et al.* tsRBase: a comprehensive database for expression and function of tsRNAs in multiple species. *Nucleic Acids Research*. 2021; 49: D1038–D1045. <https://doi.org/10.1093/nar/gkaa888>.
- [47] Green JA, Ansari MY, Ball HC, Haqqi TM. tRNA-derived fragments (tRFs) regulate post-transcriptional gene expression via AGO-dependent mechanism in IL-1 β stimulated chondrocytes. *Osteoarthritis and Cartilage*. 2020; 28: 1102–1110. <https://doi.org/10.1016/j.joca.2020.04.014>.